ISSN 0208-7774 TRIBOLOGIA 3/2018 p. 123–130

Jarosław SĘP*, Leszek TOMCZEWSKI*, Lidia GAŁDA*

STEADY-STATE ANALYSIS OF JOURNAL BEARINGS WITH HELICAL GROOVES

CHARAKTERYSTYKI STATYCZNE ŁOŻYSK ŚLIZGOWYCH ZE SPIRALNYM ROWKIEM

Key words: groove geometry, grooved journal bearings, steady-state.

Abstract

The spiral groove on the sliding journal surface enables the contaminants and eventual wear debris removal from the contact zone and bearing clearance. In this way, the wear and seizure resistance of slide bearings operating in difficult conditions became greater. The presence of a groove on bearing's surface affects the hydrodynamic performance of the bearing.

The aim of the article is to study the load carrying capacity, oil flow rate, and maximum oil temperature and pressure of slide bearings with a spiral groove at different operational conditions. Simulations were realized with the adiabatic, three-dimensional model of the oil flow in the bearing clearance. The oil flow was determined with the Navier-Stokes, continuity, and energy equations. The finite volume method was applied for calculations in ANSYS Fluent software.

As a result of the investigations, it has been stated that, with the sliding velocity increase, the load capacity also increased, but the load capacity of the grooved journal was smaller than that of plain bearings. The maximum oil temperature in the bearing clearance of grooved journal bearing was lower than that of smooth ones, and, with the sliding velocity increase, the maximum temperature also increased. The oil flow rate was greater for the grooved series than for the smooth seies at all examined velocities and clearances.

Słowa kluczowe: kształt rowka, łożysko ślizgowe z rowkiem, stan ustalony.

Streszczenie

Spiralny rowek w powierzchni ślizgowej czopa umożliwia usuwanie zanieczyszczeń ze strefy tarcia, zwiększając odporność na zatarcie i zużycie łożysk pracujących w trudnych warunkach. Modyfikacja geometrii powierzchni ślizgowej wpływa na kształt filmu olejowego w szczelinie smarowej łożyska i tym samym na charakterystyki łożyska.

Celem artykułu jest określenie nośności łożyska, wydatku oleju i temperatury występujących w łożysku ślizgowym z ukształtowanym rowkiem na powierzchni czopa przy zróżnicowanych parametrach pracy. Badania symulacyjne zrealizowano w oparciu o adiabatyczny, przestrzenny model przepływu oleju w szczelinie smarowej. Przepływ oleju został opisany równaniami Naviera-Stokesa, ciągłości i energii. Do obliczeń zastosowano metodę objętości skończonych w programie ANSYS Fluent.

W wyniku zrealizowanych badań stwierdzono, że wraz ze wzrostem prędkości poślizgu zwiększa się nośność łożysk w badanym zakresie zmienności, a nośność łożysk z rowkiem była mniejsza niż gładkich. Maksymalna temperatura oleju w szczelinie smarowej łożysk z rowkiem była niższa niż w przypadku łożysk gładkich i wraz ze zwiększeniem prędkości poślizgu maksymalna temperatura oleju również rosła. Łożyska ślizgowe z rowkiem charakteryzowały się większym wydatkiem oleju niż łożyska gładkie w całym zakresie prędkości poślizgu i przy wszystkich badanych luzach łożyskowych.

INTRODUCTION

Bearings are one of the most elementary machine elements that strongly influence its operation. Bearings enable the shaft to carry the load with the specific motion of the machine elements. The quality of bearings affects the kinematic reliability of machines. The quality assurance of machines is realized in many ways, such as special design, adequate materials, coatings, cooling systems, filters, and other solutions that depend on

* Rzeszow University of Technology, Faculty of Mechanical Engineering and Aeronautics, Powstańców Warszawy 12, 35-959 Rzeszów, Poland, e-mail: jsztmiop@prz.edu.pl.

the machine application. The meaningful factors that affect the mechanism design are connected with the environmental conditions. In case of slide bearings, the contaminants in the oil are dangerous for their proper operations. Typical slide bearings are built of hard a bushing and comparatively soft bearing, so, in situations of a high concentration of contaminants, the abrasive parts are embedded in the soft material of the bearing and scratch the bushing surface. It is difficult to eliminate the contaminants from the oil and stop the contaminants from entering the bearing clearance. If this happens, one needs to move these contaminants out of the bearing clearance by a specially created pathway. One of the design examples is a spiral groove on journal surface. Due to the spiral groove, the wear resistance of the journal bearing increased over two times in comparison to the abrasive wear of a smooth journal **[L. 1–4]**. On the other hand, the groove on the journal's surface may cause the load carrying capacity to decrease, but there are examples that grooves increased the bearing load capacity. The idea of spiral and herringbone grooves on a journal bearing surface comes from 1940's. At the beginning, in gasodynamic **[L. 5]** and later in hydrodynamic **[L. 6–8]** bearings, the grooves were created. Nowadays, grooved journal bearings are implemented in different electronic devices, because, at high speeds and low loads, the grooved journal bearings assure stable operation. Spiral groove also prevent deep scratches growing on journal bearing surfaces. It is theoretically and experimentally proved that deep scratches on shaft surfaces significantly affect the journal bearing's performance **[L. 9, 10]**. Dobrica and Fillon **[L. 9]** demonstrated that the most important parameter that influenced the pressure decrease is the scratch depth. Giraudeau et al. **[L. 10]** confirmed in the experimental tests that the scratch depth effects on pressure and temperature in the bearing clearance, but this effect depends on the applied load and speed.

The aim of this article is to study the steady-state of grooved journal bearings that were characterized in experimental tests by over a two-fold greater resistance to abrasive wear than plain journal bearings **[L. 1, 4]**.

NUMERICAL PROCEDURE

In **Fig. 1**, the scheme of the grooved journal bearing is presented. On the journal surface, the spiral groove with a specific geometry was designed. The spiral lead of the groove H was equal to 16 mm, and the area of groove cross section was 0.0223 mm^2. The width w_g of the spiral groove was 0.5 mm, and its depth d_g was 0.079 mm.

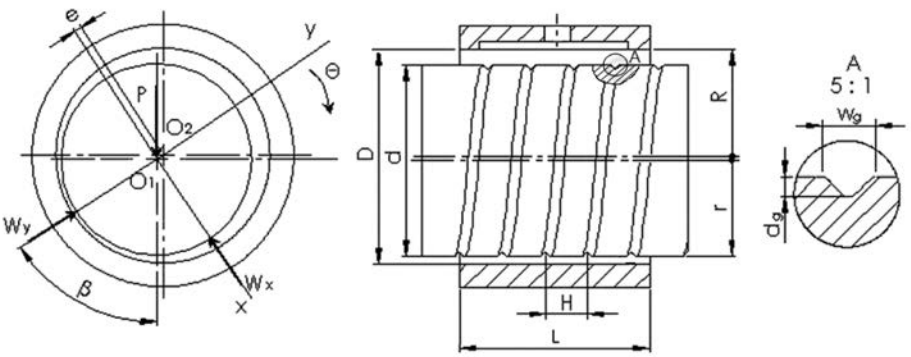

Fig. 1. Scheme of the grooved journal bearing
Rys. 1. Schemat węzła łożyskowego z czopem z rowkiem

Taking into account this problem, Navier-Stokes equations (1) describing the flows are as follows:

$$\rho\left(u_r\frac{\partial u_r}{\partial r}+\frac{u_\theta}{r}\frac{\partial u_r}{\partial \theta}-\frac{u^2{}_\theta}{r}+u_z\frac{\partial u_r}{\partial z}\right)=-\frac{\partial p}{\partial r}+\eta\left(\frac{1}{r}\frac{\partial}{\partial r}\left(r\frac{\partial u_r}{\partial r}\right)-\frac{u_r}{r^2}+\frac{1}{r^2}\frac{\partial^2 u_r}{\partial \theta^2}-\frac{2}{r^2}\frac{\partial u_\theta}{\partial \theta}+\frac{\partial^2 u_r}{\partial z^2}\right)$$

$$\rho\left(u_r\frac{\partial u_\theta}{\partial r}+\frac{u_\theta}{r}\frac{\partial u_\theta}{\partial \theta}+\frac{u_r u_\theta}{r}+u_z\frac{\partial u_\theta}{\partial z}\right)=-\frac{1}{r}\frac{\partial p}{\partial \theta}+\eta\left(\frac{1}{r}\frac{\partial}{\partial r}\left(r\frac{\partial u_\theta}{\partial r}\right)-\frac{u_\theta}{r^2}+\frac{1}{r^2}\frac{\partial^2 u_\theta}{\partial \theta^2}+\frac{2}{r^2}\frac{\partial u_r}{\partial \theta}+\frac{\partial^2 u_\theta}{\partial z^2}\right) \quad (1)$$

$$\rho\left(u_r\frac{\partial u_z}{\partial r}+\frac{u_\theta}{r}\frac{\partial u_z}{\partial \theta}+u_z\frac{\partial u_z}{\partial z}\right)=-\frac{\partial p}{\partial z}+\eta\left(\frac{1}{r}\frac{\partial}{\partial r}\left(r\frac{\partial u_z}{\partial r}\right)+\frac{1}{r^2}\frac{\partial^2 u_z}{\partial \theta^2}+\frac{\partial^2 u_z}{\partial z^2}\right)$$

To solve the problem, the mass continuity (2), energy (3), and the function of energy dissipation (4) equations were also applied:

$$\frac{1}{r}\frac{\partial(ru_r)}{\partial r}+\frac{1}{r}\frac{\partial(u_\theta)}{\partial \theta}+\frac{\partial u_z}{\partial z}=0 \qquad (2)$$

$$\rho c\left(u_r\frac{\partial T}{\partial r}+\frac{u_\theta}{r}\frac{\partial T}{\partial \theta}+u_z\frac{\partial T}{\partial z}\right)=k\left(\frac{1}{r}\frac{\partial}{\partial r}\left(r\frac{\partial T}{\partial r}\right)+\frac{1}{r^2}\frac{\partial}{\partial \theta}\left(\frac{\partial T}{\partial \theta}\right)+\frac{\partial}{\partial z}\left(\frac{\partial T}{\partial z}\right)\right)+\eta\Phi \qquad (3)$$

$$\Phi=\left\{2\left[\left(\frac{\partial u_r}{\partial r}\right)^2+\left(\frac{\partial u_\theta}{\partial r}\right)^2+\left(\frac{\partial u_z}{\partial r}\right)^2\right]+\left(\frac{1}{r}\frac{\partial u_r}{\partial \theta}+\frac{\partial u_\theta}{\partial r}\right)^2+\left(\frac{\partial u_\theta}{\partial z}+\frac{1}{r}\frac{\partial u_z}{\partial \theta}\right)^2+\left(\frac{\partial u_z}{\partial r}+\frac{\partial u_r}{\partial z}\right)^2\right\} \qquad (4)$$

The total load carrying capacity W [N] was calculating by integrating the pressure field along the journal bearing surface using Formulas (5)–(7):

$$W=\sqrt{(W_x)^2+(W_y)^2},\qquad where \qquad (5)$$

$$W_x=r\int_0^L\int_0^{\theta_k} p\,\sin\Theta d\Theta dz \qquad (6)$$

$$W_y=r\int_0^L\int_0^{\theta_k} p\,\cos\Theta d\Theta dz \qquad (7)$$

The oil viscosity η strongly affects the load carrying capacity of the bearing. The variations of the viscosity with the temperature changes were examined and the measured values were introduced into the calculation procedure. The effect of temperature on the oil density ρ was also tested experimentally and the obtained values were input for the software. The oil viscosity and density were also obtained as regression functions of temperature (8 and 9):

$$\eta=4\cdot10^{28}\cdot T^{-12.02}\quad [\text{Pa·s}] \qquad (8)$$

$$\rho=-0.0071\cdot T^2+3.9143\cdot T+341.07\quad [\text{kg/m}^3] \qquad (9)$$

The pressure at the oil inlet and on both sides of the bearing were defined as the boundary conditions in calculations and set to ambient temperature at the oil inlet (293 K) (**Fig. 2**). The sliding speed was changed from 0.55 to 4.41 m/s (200–1600 rpm) for selected eccentricity ε equal to 0.76. Iterations were run until the convergence index was reached or calculations were stopped after 500 iterations.

The geometrical dimensions of the simulated journal bearings are the same as in previous experimental tests **[L. 1–4]** conducted in the contaminated oil. In presented numerical simulations, the clean oil was modelled to investigate the one optimum grooved series (optimum in abrasive wear resistance), taking into account the groove geometry according to the load carrying capacity W [N], maximum temperature T [K], oil flow rate q_0 [kg/s], and maximum oil pressure p_{max} [Pa] and to compare them with the results obtained in case of a smooth bearing. The bearing geometry and the mineral oil L-AN 46 properties of the modelled bearing clearance are presented in **Tab. 1**.

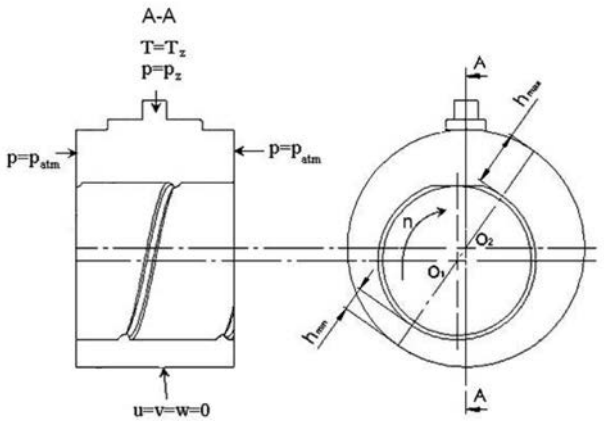

Fig. 2. Modelled bearing clearance (series with spiral groove) with boundary conditions

Rys. 2. Model szczeliny smarowej (wariant z rowkiem na czopie) i warunki brzegowe

Table 1. The bearing geometry and the oil L-AN 46 properties of modelled bearing clearance

Tabela 1. Geometria łożyska i właściwości oleju L-AN 46 w modelowanej szczelinie smarowej

Bearing diameter	D	52.8 mm
Shaft diameter	D	52.7 mm
Bearing length	L	30 mm
Lubricant supply temperature	Tz	293 K
Kinematic viscosity	υ	46 $mm^2\ s^{-1}$ at 40ºC
Specific heat of lubricant	c	2000 $J\ kg^{-1}\ K^{-1}$
Thermal conductivity of lubricant	k	0.145 $W\ m^{-1}\ K^{-1}$

A model of the bearing clearance was prepared with the program ANSYS 16.2 for numerical calculations based on the finite volume method and with some user defined applications. In **Fig. 3**, the finite elements grids of the clearance and feeding groove in the smooth (**Fig. 3a**) and grooved journal bearings (**Fig. 3b**) are presented. There were 12 elements in the height of the bearing clearance. The higher densities of finite elements in the circumferential direction of the meshed clearance were introduced in groove zones (**Fig. 3b**). According to **[L. 11]**, the grid of the grooved zone was five-times denser in the circumferential direction than it was in the smooth zone. The models were comprised of almost 1 million elements in the case of smooth bearing clearance and over 1.6 million elements of clearance in the grooved journal bearing. The mesh quality of the smooth and grooved models were satisfied because the orthogonal quality was higher than 0.1 and the skewness was close to zero (**Tab. 2**).

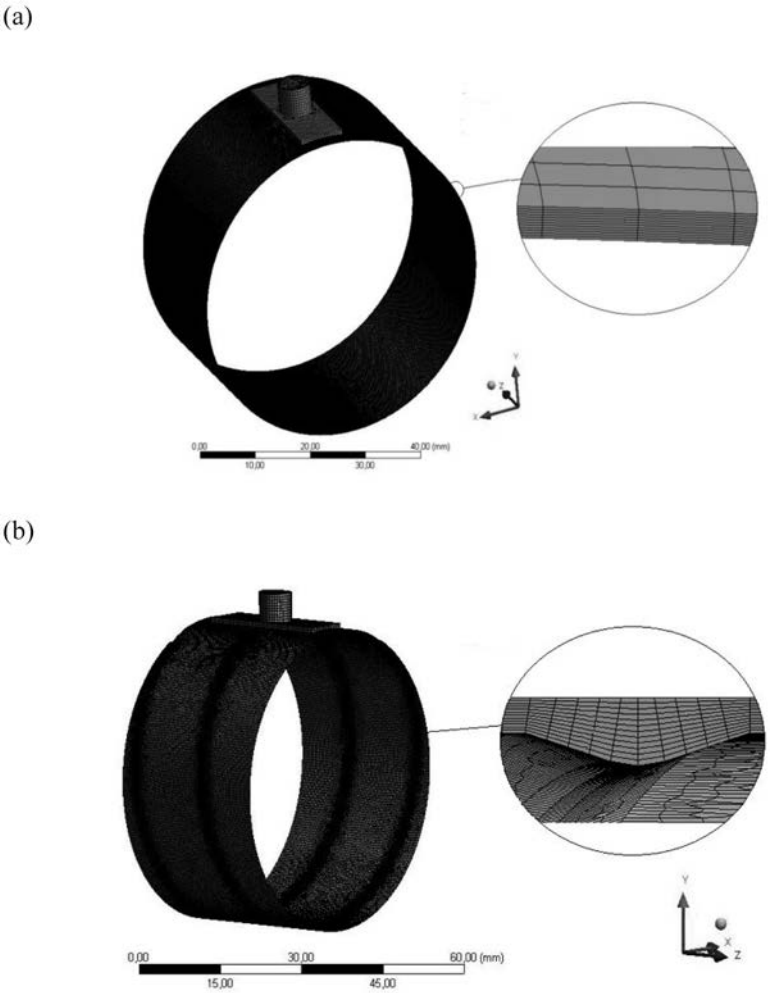

Fig. 3. Finite elements grids of clearance in smooth (a) and grooved (b) journal bearings

Rys. 3. Siatka elementów skończonych szczeliny smarowej w łożysku gładkim (a) i z rowkiem (b)

Table 2. Grids parameters of smooth and grooved bearing clearance

Tabela 2. Parametry siatki szczeliny smarowej łożyska gładkiego i z rowkiem

Parameter	Smooth	Grooved
Elements number	918296	1661349
Nodes number	1007016	1530857
Orthogonal quality: min (average)	0.363 (0.985)	0.13 (0.9)
Skewness: min (average)	$1.86 \cdot 10^{-3}$ ($2.78 \cdot 10^{-3}$)	$2.2 \cdot 10^{-6}$ (0.19)

RESULTS AND DISCUSSION

As the result of numerical investigations, some characteristics of grooved and smooth journal bearings with different bearing clearances in the range of sliding velocity 0.55 – 4.41 m/s were obtained. The maximum oil temperature in the bearing clearance depends on the sliding velocity of the moving element. The graphs of the temperature courses via speed values are presented in **Fig. 4**.

Temperature values increased with the increase of sliding speed. The series with the biggest relative clearance (ψ = 0.003) was characterized by small deviations from the linear course of temperature values. Generally, lower temperature values were achieved when

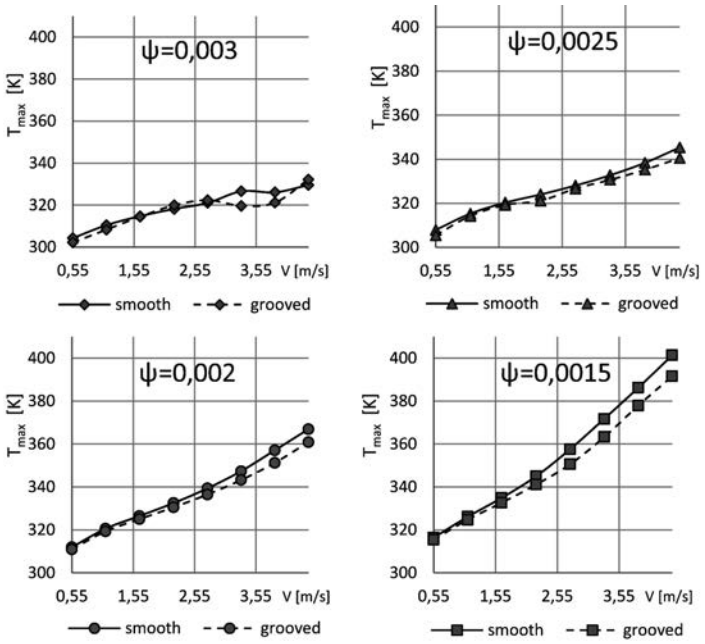

Fig. 4. The influence of sliding speed V [m/s] on the maximum oil temperature T_{max} [K] at different relative bearing clearance for smooth and grooved journals

Rys. 4. Wpływ prędkości poślizgu V [m/s] na maksymalną wartość temperatury oleju T_{max} [K] przy zróżnicowanym względnym luzie łożyskowym dla łożysk gładkich i z rowkiem

the spiral groove was on journal surface, which enabled cooling the oil. The smaller the relative clearance ψ the higher was the maximum temperature of the oil. When decreasing the relative clearance from 0.003 to 0.0015, the 21% increase in the maximum oil temperature at the greatest sliding velocity of 4.41 m/s was obtained, but the groove application decreased the maximum temperature by 10 K.

With the speed increase, the oil flow rate also increased, and the most dynamic growth was achieved for the highest clearance series 0.003. Flow rate as a dependence with the velocity is presented in **Fig. 5**.

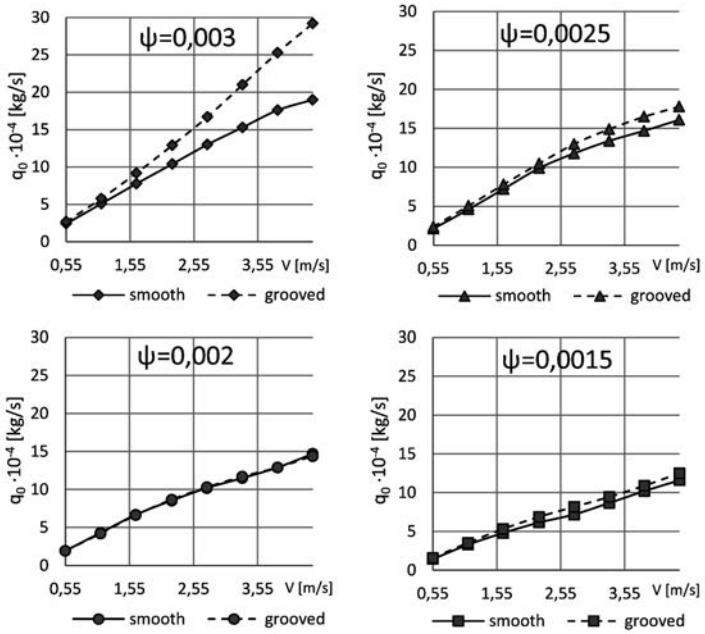

Fig. 5. The influence of sliding speed V [m/s] on flow rate q_0 [kg/s] at different relative bearing clearance for smooth and grooved journals

Rys. 5. Wpływ prędkości poślizgu V [m/s] na wydatek oleju q_0 [kg/s] przy zróżnicowanym względnym luzie łożyskowym dla łożysk gładkich i z rowkiem

The flow rate values also decreased with the decrease of clearance. The higher flow rate was obtained when the groove was created on the journal in most examined cases, but the differences were not great when the clearance was small. The greater flow rate in the case of grooved journals enables the intake of cooler lubricant from the system and keeps the higher viscosity of the oil which influences the load carrying capacity of the journal bearing. But the load capacity W was larger for conventional bearings almost for all courses of examined cases (**Fig. 6**). The exception was the series of $\psi = 0.003$, which, at higher speeds, indicated that the load carrying capacity of grooved journal was higher than that of the smooth one, but it could be an imperfection of the model that is demonstrated in these operating conditions. Courses of the bearing capacity are similar in the shape to the pressure courses with some stages of increased and stable values. The load carrying capacity of the grooved journal was mainly lower than that of the smooth bearing when the clean oil was taken into account, but this should not be the only criterion for the journal bearing design. The sliding bearings do not operate in clean oil, but lubricating substances usually contain contaminants and wear debris, and the simulation with clean oil is treated as the initial step considered in the design process. Often, the more important criteria are connected with practical application and environmental conditions. The final solution of bearing design is the consensus reached after many factors are analysed.

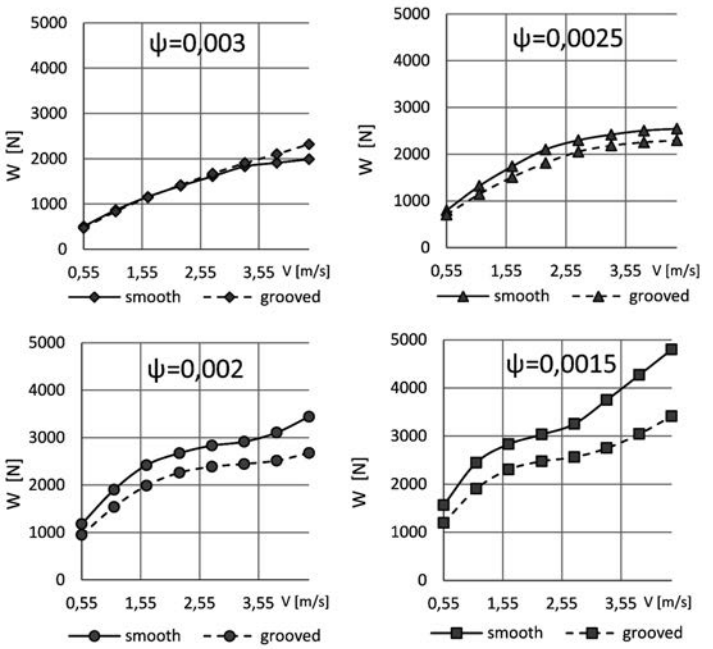

Fig. 6. The influence of sliding speed V [m/s] on load carrying capacity W [N] at different relative bearing clearance for smooth and grooved journals

Rys. 6. Wpływ prędkości poślizgu V [m/s] na nośność W [N] przy zróżnicowanym względnym luzie łożyskowym dla łożysk gładkich i z rowkiem

In **Fig. 7**, maximum pressure values of the oil film in relation to the sliding velocities in the range of 0.55 – 4.41 m/s are presented. With the increase in speed, the maximum pressure mainly increased. At the greatest bearing clearance, the pressure values were the smallest. The max pressure of the series with a relative clearance $\psi = 0.0025$ increased with the velocity increase, but after 2.55 m/s, it stabilized. The series with the small clearances of $\psi = 0.002$ and $\psi = 0.0015$, after an initial increase and stabilization period, were characterized with a further increase in maximum pressure values. The smooth journal bearing obtained higher pressure values in comparison to grooved bearings, which generally correlated with other results. However, one exception was found at $\psi = 0.003$, where, at higher speeds, the grooved bearing obtained greater maximum oil pressure. It is hard to explain, but the model probably was inaccurate enough in these conditions. The greatest differences in pressure values were observed mainly at the high velocities and at small clearances.

The decrease in the pressure due to the creation of the spiral groove on the journal surface was up to 27%.

The load carrying capacity of the journal bearing with a spiral groove is lower than that of a smooth journal surface, but this specific channel creates mitigation to the presence of contaminants **[L. 1–4]**. Moreover, the possibility for the cooling of the bearing system is greater because the lubricating substance

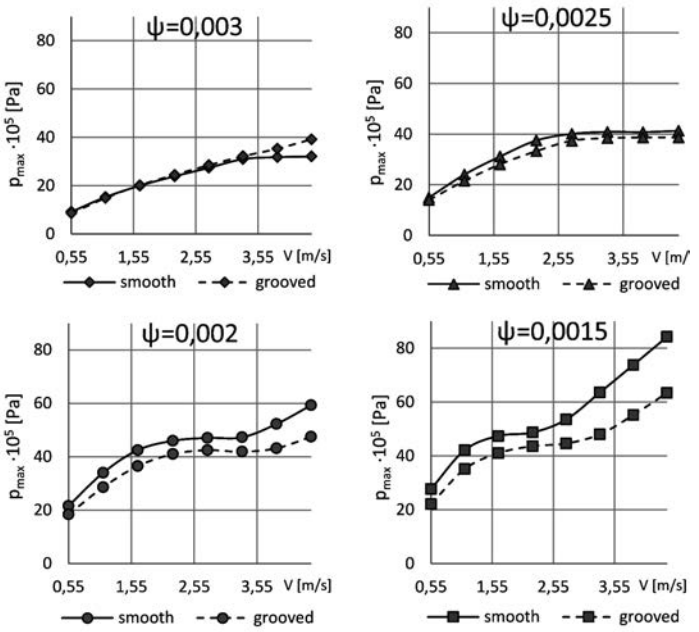

Fig. 7. The influence of sliding speed V [m/s] on max pressure p_{max} [Pa] at different relative bearing clearance for smooth and grooved journals

Rys. 7. Wpływ prędkości poślizgu V [m/s] na maksymalną wartość ciśnienia p_{max} [Pa] przy zróżnicowanym względnym luzie łożyskowym dla łożysk gładkich i z rowkiem

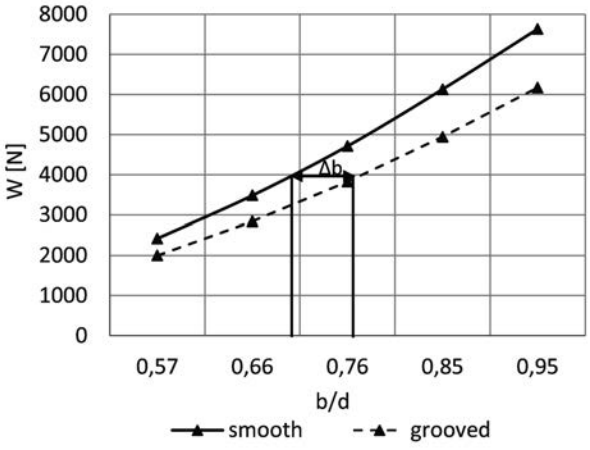

Fig. 8. The influence of bearing length ratio b/d on load carrying capacity W [N]

Rys. 8. Wpływ współczynnika długości łożyska b/d na nośność W [N]

is transported through the grooves out of the working zone. The disadvantage of the load carrying capacity decrease may be compensated by an increase in bearing length. In **Fig. 8**, there is example of how to obtain the same value of the load bearing capacity of conventional and grooved journal bearing. The 8% increase of bearing length from grooved journal bearing allowed achieving the same bearing capacity as that of a smooth bearing. The extension the bearing dimension needs further examination to check how other characteristics change.

CONCLUSIONS

The helical groove on journal surface influenced the bearing characteristics in steady-state. Load carrying capacity simulated at varied sliding velocities in the range of 0.55–4.41 m/s was generally lower when the groove was present on the shaft, but the maximum oil temperature decreased due to greater fluid flow rate. The greatest decrease in load carrying capacity caused by the groove presence was found when the bearing clearance was the smallest $\psi = 0.0015$ and the velocity was the highest 4.41 m/s. The highest increase in oil flow rate due to groove creation was found for the greatest bearing clearance and the biggest sliding velocity, but, in this case, the maximum oil temperature values were quite similar for both the smooth and grooved series.

Because the grooved journal bearing has great abrasive resistance, in some situations, this design may be successfully implemented, and the eventual decrease in load carrying capacity can be compensated by increasing the bearing length by a percentage of the total length.

REFERENCES

1. Sęp J., Pawlus P., Gałda L.: The effect of helical groove geometry on journal abrasive wear. Archives of Civil and Mechanical Engineering 13, pp. 150–157 (2013).
2. Sęp J.: Selected properties of bearings with helical groove on the journal, Key Engineering Materials 490, pp. 273–281 (2012).
3. Sęp J., Pawlus P., Dzierwa A.: The analysis of abrasive wear of the helical grooved journal bearing. Key Engineering Materials 527, pp. 173–178 (2013).
4. Sęp J., Tomczewski L., Gałda L., Dzierwa A.: The study on abrasive wear of grooved journal bearings. Wear 376–377, pp. 54–62 (2017).
5. Vohr J.H., Chow C.Y.: Characteristics of herringbone-grooved, gas-lubricated journal bearings. Transactions of the ASME, Journal of Basic Engineering, vol. 87, pp. 568–578 (1965).
6. Bootsma J.: The gas liquid interface and the load capacity of helical grooved journal bearings, Transactions of the ASME, Journal of Lubrication Technology 95, pp. 94–100 (1973).
7. Bootsma J., Tielemans L.P.M.: Conditions of leakage-free operation of herringbone grooved journal bearings, Transactions of the ASME, Journal of Lubrication Technology 99, pp. 215–223 (1977).
8. Hirs G.G.: The load capacity and stability characteristics of hydrodynamic grooved journal bearings. ASLE Transactions, vol. 8, pp. 296–305 (1965).
9. Dobrica M., Fillon M.: Performance degradation in scratched journal bearing. Tribology International 51, pp. 1–10, (2012).
10. Giraudeau C., Bouyer J., Fillon M., Helene M., Beaurian J.: Experimental study of the influence of scratches on the performance of a two-lobe journal bearing. STLE Tribology Transactions vol. 60, no. 5, pp. 942–955 (2017).
11. Etsion I.: Modeling of surface texturing in hydrodynamic lubrication. Friction 1 (3), pp. 195–209 (2013).